

A WINDOWED DIGRAPH FOURIER TRANSFORM

Rasoul Shafipour[†], Ali Khodabakhsh[‡], and Gonzalo Mateos[†]

[†]Dept. of Electrical and Computer Engineering, University of Rochester, Rochester, NY, USA

[‡]Dept. of Electrical and Computer Engineering, University of Texas at Austin, Austin, TX, USA

ABSTRACT

We propose a methodology to carry out vertex-frequency analyses of graph signals, with the goal of unveiling the signal's frequency occupancy over a localized region in the network. To this end, we first introduce localized graph signals in the vertex domain, by defining windows that are localized around each node by construction. Recent directed graph Fourier transform (DGFT) advances facilitate the frequency analysis of said localized signals, to reveal the signal's energy distribution in a way akin to a spectrogram in the vertex-frequency plane. We then learn a set of windows by applying gradient descent method to an optimization problem governed by penalty parameters in the spectral domain. We also argue about the tradeoff between the resolution in the vertex and frequency domains based on the said parameters. We evaluate the performance of the proposed windowed GFT approach through numerical experiments on synthetic and real-world graphs.

Index Terms— Graph signal processing, windowed graph Fourier transform, vertex-frequency analysis, directed graphs.

1. INTRODUCTION

Network data indexed by the nodes of a graph are becoming increasingly ubiquitous, with examples ranging from measurements of neural activities at different regions of the brain [1,2], to economic activity observed over a network of production flows between industrial sectors [3]. Predicated on the assumption that the properties of a network process relate to the underlying graph, the goal of graph signal processing (GSP) is to broaden the scope of traditional signal processing tasks and develop algorithms that fruitfully exploit this relational structure; see [4,5] for tutorial treatments. From this vantage point, signal processing tasks such as filtering [2,5–8], sampling and reconstruction [3,9–11], spectrum estimation [12], (blind) filter identification [13,14], as well as signal representations [15,16], have been reexamined under the purview of GSP.

An instrumental GSP tool is the graph Fourier transform (GFT), which decomposes a graph signal into orthonormal components describing different modes of variation with respect to the graph topology [4,17]. Similar to the classical Fourier-related transforms which could not capture the time-varying properties, GFT obscures the dependency on the vertices. However, short-time (aka windowed) Fourier transforms (STFT) with broad applications (e.g., speech analysis) have well-documented merits in extracting time-frequency contents from signals with localized oscillations in time or space. To enable vertex-frequency analysis, here we aim to generalize windowed Fourier analysis to both undirected and directed graphs (digraphs); see also [18,19]. We build on a novel digraph (D)GFT which provides an orthonormal basis, where each basis vector captures a different (directed) variation and the resulting frequencies (i.e., the directed variation of the sought orthonormal

basis vectors) distribute as evenly as possible across the viable spectrum. We generalize the localization operator in the vertex domain by learning (smooth) windows which highlight the signal values in prescribed neighborhoods. Then we introduce the windowed (W)GFT as a function of frequency and spatial location of window by taking the DGFT of the localized signals. The proposed WGFT can facilitate more interpretable vertex-frequency analyses.

To position our contributions in the context of related work, we first introduce some basic GSP notions and terminology. We consider a weighted digraph $\mathcal{G} = (\mathcal{V}, \mathbf{A})$, where \mathcal{V} is the set of nodes (i.e., vertices) with cardinality $|\mathcal{V}| = N$, and $\mathbf{A} \in \mathbb{R}^{N \times N}$ is the graph adjacency matrix with entry A_{ij} denoting the edge weight from node j to node i . We assume that the graph is connected and has no self loops; i.e. $A_{ii} = 0$, and the edge weights are non-negative ($A_{ij} \geq 0$). For an undirected graph \mathbf{A} is symmetric, and the positive semi-definite combinatorial Laplacian matrix is $\mathbf{L} := \mathcal{D} - \mathbf{A}$, where \mathcal{D} is the diagonal degree matrix with $\mathcal{D}_{ii} = \sum_j A_{ji}$. A graph signal $\mathbf{x} : \mathcal{V} \mapsto \mathbb{R}^N$ can be represented as a vector of size N , where component x_i denotes the signal value at node $i \in \mathcal{V}$.

Related work. For undirected graphs, the GFT of signal \mathbf{x} is often defined as $\tilde{\mathbf{x}} = \mathbf{V}^T \mathbf{x}$, where $\mathbf{V} := [\mathbf{v}_1, \dots, \mathbf{v}_N]$ comprises the eigenvectors of the Laplacian [4,8]. Defining the total variation of the signal \mathbf{x} with respect to the Laplacian \mathbf{L} as

$$\text{TV}(\mathbf{x}) = \mathbf{x}^T \mathbf{L} \mathbf{x} = \sum_{i,j=1, j>i}^N A_{ij} (x_i - x_j)^2 \quad (1)$$

then it follows that the total variation of eigenvector \mathbf{v}_k is $\text{TV}(\mathbf{v}_k) = \lambda_k$, the k^{th} Laplacian eigenvalue. Hence, eigenvalues $0 = \lambda_1 < \lambda_2 \leq \dots \leq \lambda_N$ can be viewed as graph frequencies, indicating how the GFT bases vary over the graph.

A generalization of STFT to graph domain is through the definition of translation and modulation operators [18]. While modulation can be interpreted by multiplication with a Laplacian eigenvector, translation (shifting to a certain node) is not well defined in the graph domain. In [18], the windowed GFT is defined as the inner product of a signal with the translated and modulated window, where translation is interpreted as a generalized convolution with delta function. While the k^{th} modulation operator ensures that a localized signal around λ_0 in the graph spectral domain will be localized around the eigenvalue λ_k in the same domain, in general the translation operator fails to localize the signal in the vertex domain. Also, the method in [18] does not inherently extend to digraphs.

To ensure that the translation operator shares key properties with the classical time shift, an isometric graph translation operator was proposed in [20] which is described in the spectral domain as a phase shifting operator. Although the isometric operator preserves the signal's energy and can be seen as linear convolution, it still does not localize the translated signal around the target node.

It is worth mentioning that the adjacency matrix itself can be viewed as a graph shift operator which is valid for digraphs as well

Work in this paper was supported by the NSF awards CCF-1750428 and ECCS-1809356.

[5]. The graph shift is an analogy to periodic signals in time, on an unweighted directed cycle. With this consideration, one application of the graph shift is the same as shifting the periodic signal by one unit in time. However, graph shift operator is not localization invariant as well.

Contributions. Here we design a WGFT with the following desirable properties: P1) The windows are localized by construction and extract the information around a prescribed vertex neighborhood. P2) Windows are smooth so as not to add undesired frequencies to the windowed signals. P3) The WGFT mimics the behavior of the traditional STFT and the vertex-frequency resolution can be tuned by changing one parameter. To that end, we first review the STFT and DGFT as our foundation in Section 2. Then we introduce WGFT in Section 3 and study the task of parametric window learning and behavior of the stationary solutions. Finally, we show the effectiveness of the proposed approach in vertex-frequency analyses in Section 4. Concluding remarks are given in Section 5.

2. FOUNDATION AND PRELIMINARIES

In this section, first we briefly review the classical short-time Fourier transform which later we follow the analogies to construct a windowed DGFT. Then, we elaborate how to find a basis for the general digraphs to fruitfully represent the graph signals in the spectral domain.

2.1. Classical short-time Fourier transform (STFT)

The short-time Fourier transform (STFT) has shown remarkable success in classical signal processing in revealing the frequency (and phase) content of localized versions of the signal around different times. This is especially important when the spectral content (e.g., DFT) of the (non-stationary) signal (e.g., speech) changes over time. Towards that end, for a signal $x(t)$, an analysis window $w(t)$ which is normally low-pass with a certain band τ ms is considered. Then the windowed segments of the signal around time i , are generated as $x^{(i)}(t) := x(t)w(t-i)$, where $w(t-i)$ is the shifted version of the window by i units. Finally, the STFT of the signal takes the form

$$\mathbf{X}(f, i) = \mathcal{F}\{x^{(i)}(t)\}, \quad (2)$$

where \mathcal{F} is a Fourier-related transform like DFT or FFT.

It is worth mentioning that the window is commonly smooth to avoid unnatural discontinuities in the segmented signal $x^{(i)}(t)$. Also, the window band τ trades off the spatial and frequency localization. As we increase τ , we are less likely to add unwanted frequency content to $x^{(i)}(t)$, so we have a better frequency resolution while we compromise the spatial localization of $\mathbf{X}(f, i)$.

2.2. Digraph Fourier transform

Recently, we have proposed a digraph Fourier transform which captures low, medium and high frequencies with respect to the digraph [21]. To that end, we collect the desired basis signals in a matrix $\mathbf{U} := [\mathbf{u}_1, \dots, \mathbf{u}_N] \in \mathbb{R}^{N \times N}$, where $\mathbf{u}_k \in \mathbb{R}^N$ represents the k th frequency component. This means that the DGFT of a graph signal \mathbf{x} is $\tilde{\mathbf{x}} = \mathbf{U}^T \mathbf{x}$. The inverse DGFT is $\mathbf{x} = \mathbf{U} \tilde{\mathbf{x}} = \sum_{k=1}^N \tilde{x}_k \mathbf{u}_k$, which allows one to synthesize \mathbf{x} as a linear combination of orthogonal frequency modes \mathbf{u}_k .

To measure how the basis \mathbf{u} varies over the network and define graph frequencies, we adopt the notion of signal directed variation (DV) over digraphs

$$\text{DV}(\mathbf{u}) := \sum_{i,j=1}^N A_{ij} [u_i - u_j]_+^2, \quad (3)$$

where $[x]_+ = \max(0, x)$ [17]. In the undirected case, DV boils down to the total variation; i.e., TV in (1). One can then define the frequency $f_k := \text{DV}(\mathbf{u}_k)$ as the directed variation of the basis \mathbf{u}_k . To cover the whole spectrum of variations, we set $\mathbf{u}_1 = \mathbf{u}_{\min} = \frac{1}{\sqrt{N}} \mathbf{1}_N$ for capturing the minimum frequency (i.e., DC component) and $\mathbf{u}_N = \mathbf{u}_{\max} := \arg \max_{\|\mathbf{u}\|_2=1} \text{DV}(\mathbf{u})$, where $f_{\max} := \text{DV}(\mathbf{u}_{\max})$ is the maximum attainable directed variation which can be found via [17, Algorithm 1]. As a criterion for the design of the remaining basis vectors, we consider the spectral dispersion function

$$\delta(\mathbf{U}) := \sum_{i=1}^{N-1} [\text{DV}(\mathbf{u}_{i+1}) - \text{DV}(\mathbf{u}_i)]^2 \quad (4)$$

that measures how well spread the corresponding frequencies $f_k = \text{DV}(\mathbf{u}_k)$ are over $[0, f_{\max}]$. Having fixed the first and last columns of \mathbf{U} , it follows that $\delta(\mathbf{U})$ is minimized when the free directed variation values form an arithmetic sequence between $f_1 = 0$ and $f_N = f_{\max}$, yielding maximally-spread frequency modes as in the DFT.

Consolidating all the criteria, learning the DGFT as the first step for finding a basis for developing WGFT can be stated as

$$\begin{aligned} \min_{\mathbf{U}} \quad & \delta(\mathbf{U}) \\ \text{subject to} \quad & \mathbf{U}^T \mathbf{U} = \mathbf{I}_N, \mathbf{u}_1 = \mathbf{u}_{\min}, \mathbf{u}_N = \mathbf{u}_{\max}. \end{aligned} \quad (5)$$

Problem (5) is feasible (i.e., $\mathbf{u}_{\max} \perp \mathbf{u}_{\min}$) as shown in [17, Proposition 3]. Stationary solutions of (5) can be found by bringing to bear a feasible method for optimization of differentiable functions over the Stiefel manifold (see [17, Algorithm 2]).

In the next section, we introduce windowing signals that are localized by construction and decay around prescribed nodes as a function of decay rates and evaluated proximity measures. Then the windowed signal around an arbitrary node is considered as the entry-wise product of the signal and the window centered around the same node. Finally, the resulting orthonormal basis \mathbf{U} of (5) is used to: (i) find the WGFT as the Fourier transform of a windowed signal; and (ii) learn the decay rates with the controllable vertex-frequency resolution via examining the smoothness of the candidate windows.

3. LEARNING SMOOTH LOCALIZED WINDOWS

Here we show how to find windowed GFT similar to the ones in classical signal processing.

Windowed GFT. To formally state our problem, let $\mathbf{D} \in \mathbb{R}_+^{N \times N}$ store the nonnegative entries D_{ji} denoting the (directed) proximities or topological structure of the graph from node i to node j . As a convention, we set the diagonal entries of \mathbf{D} to zero. For example, D_{ji} can be the length of the shortest path from node i to node j . Given \mathbf{D} , we seek a (smooth) window in the vertex domain that is localized around a prescribed vertex. To that end, we define a window around node i as a graph signal with value one at node i and value being inversely proportional with d_{ji} at node j . Upon defining the vector of decay rates $\boldsymbol{\tau} = [\tau_1, \dots, \tau_N] \in \mathbb{R}_+^N$ for the nodes of the graph, the windowing signal $\phi_i \in \mathbb{R}^N$ around node i can have the entries following e.g., an exponential decay $\phi_{ji} = \exp(-\tau_i d_{ji})$ or a power law relationship $\phi_{ji} = d_{ji}^{-\tau_i}$ for $j \in [N] = \{1, \dots, N\}$. While the proposed framework can be applied to any decaying differentiable window, here we consider the exponential window for simplicity. Also, let $\boldsymbol{\Phi} = [\phi_1, \dots, \phi_N] = [\phi_{ji}] \in \mathbb{R}^{N \times N}$ collect the vertices decay functions.

Then we define the windowed (localized) signal $\mathbf{x}^{(i)}$ around node i as

$$\mathbf{x}^{(i)} := \mathbf{x} \circ \phi_i = \text{diag}(\mathbf{x}) \phi_i, \quad (6)$$

where \circ is the element-wise product, and $\text{diag}(\mathbf{x})$ is a diagonal matrix with entries of \mathbf{x} on the diagonal. To be more specific, the i th element of $\mathbf{x}^{(i)}$ is the same as x_i , while the other elements are attenuated based on their distance from node i . To preserve the energy of the signal, one can normalize $\mathbf{x}^{(i)}$ to have the same norm as \mathbf{x} .

Similar to traditional STFT (see Section 2.1), we define the windowed (D)GFT as

$$\tilde{\mathbf{X}} = [\tilde{\mathbf{x}}^{(1)}, \dots, \tilde{\mathbf{x}}^{(N)}] := [\mathbf{U}^T \mathbf{x}^{(1)}, \dots, \mathbf{U}^T \mathbf{x}^{(N)}] \quad (7)$$

$$= \mathbf{U}^T \text{diag}(\mathbf{x}) \Phi,$$

where basis \mathbf{U} is obtained by solving (5).

The entry $\tilde{\mathbf{X}}(f, i)$ in (7) represents the frequency content of node i in the f th frequency component. For example, by examining the f th row of $\tilde{\mathbf{X}}$ one can infer the vertices (or the neighborhoods) contributing more to the f th frequency through detecting the corresponding entries having the largest magnitude. Likewise, one can explore column-wise to find out activated frequencies in a neighborhood.

Learning windows. To estimate the parameters embedded in the decay matrix Φ , one can impose desirable spectral characteristics. We would like to find smooth windows capturing the locality, similar to the STFT. To enforce the smoothness, we define a weight vector $\mathbf{w} = [w_1, \dots, w_N]^T \in \mathbb{R}_+^N$ that penalizes the window for having high frequency components. In addition to high frequency components, we should also prevent the window from picking the first component (constant signal), as it will not be local. We then solve the following optimization problem:

$$\min_{\tau \in \mathbb{R}_+^N} \frac{1}{2} \|\text{diag}(\mathbf{w}) \mathbf{U}^T \Phi\|_F^2 = \frac{1}{2} \sum_{i=1}^N \|\text{diag}(\mathbf{w}) \mathbf{U}^T \phi_i\|_2^2. \quad (8)$$

For the choice of w_i 's we can set $w_i = h(\text{DV}(\mathbf{u}_i))$ for $i \geq 2$, where h is a monotone increasing function. We resort to a linear function h , but one can use convex functions to further penalize the high frequency components. Furthermore for w_1 , there is a tradeoff between the resolution in vertex and spectral domains, as we formally prove in Proposition 2. In the extreme case if we set $w_1 = 0$, then the optimal τ_i will be zero but it yields a constant window of $\phi_{ji} = 1$ for all j (see Proposition 1). Despite being smooth, this window does not capture the desired locality property and we lose the resolution in vertex domain. On the other hand as we increase w_1 , the optimal τ_i increases. This drives the window towards Dirac delta function, which has the best locality in the vertex domain, but it creates undesirable frequencies due to its non-smooth character. In other words, we lose the resolution in frequency domain.

Note that in (8), each τ_i only appears in ϕ_i . Therefore the above optimization problem breaks into N independent subproblems. Let $f_i(\tau_i)$ be the i th term of the summation in (8), then each subproblem is of the following form:

$$\min_{\tau_i \geq 0} f_i(\tau_i) = \frac{1}{2} \|\text{diag}(\mathbf{w}) \mathbf{U}^T \phi_i\|_2^2. \quad (9)$$

We use gradient descent method to solve each subproblem. Let $\mathbf{W} = \text{diag}([w_1^2, \dots, w_N^2])$, then the gradient of f_i with respect to τ_i takes the form

$$g = df_i = -(\mathbf{d}_i \circ \phi_i)^T \mathbf{U} \mathbf{W} \mathbf{U}^T \phi_i. \quad (10)$$

Then the update rule of gradient descent method boils down to (superscript $k = 1, 2, \dots$ denotes iterations)

$$\tau^{k+1} = \tau^k - \eta^k g(\tau^k), \quad (11)$$

where $\eta^k > 0$ is the step size that can be picked properly such that it guarantees the convergence to a stationary point, which we next prove its existence in the nonnegative reals through Proposition 1 and Proposition 2.

Proposition 1 *If $w_1 = 0$, then the optimal value of (9) is zero and is achieved by $\tau_i = 0$, i.e., $f_i(0) = 0$.*

Proof: Note that the norm in (9) can be written as

$$\|\text{diag}(\mathbf{w}) \mathbf{U}^T \phi_i\|_2^2 = \sum_{i=1}^N (w_i \mathbf{u}_i^T \phi_i)^2.$$

For $\tau_i = 0$, the window ϕ_i turns to all ones vector, hence $\phi_i = \sqrt{N} \mathbf{u}_1$. This implies that $\mathbf{u}_i^T \phi_i = 0$ for $i \geq 2$. The first term of the summation is also zero because $w_1 = 0$. Since f_i is non-negative, this completes the proof. ■

Proposition 1 implies that $w_1 = 0$ results in $\tau = 0$ which corresponds to the constant all ones window. In that case, WGFT boils down to DGFT and we do not gain any resolution in the vertex domain. Next, we prove that as we increase w_1 and make it further apart from zero, τ would also increase which compromises the frequency resolution in WGFT for more resolution in vertex domain.

Proposition 2 *Let w_1, w'_1 be two parameters for penalizing the DC component of the window such that $w_1 < w'_1$ (while we keep the other penalty parameters unchanged). If τ is a local minima for the optimization problem (9) with w_1 , then the corresponding optimization problem for w'_1 has a local (or asymptotic) minima $\tau' \in (\tau, +\infty) \cup \{+\infty\}$.*

Proof: Observe that $f_i(\tau_i)$ is lower bounded by zero. Therefore, to prove that $\tau < \tau'$ it suffices to show that $g'(\tau) < 0$, where g' is the gradient for the subproblem with w'_1 . We can write the gradient (10) as

$$g'(\tau) = -(\mathbf{d}_i \circ \phi_i)^T \left(\sum_{j=1}^N w_j'^2 \mathbf{u}_j \mathbf{u}_j^T \right) \phi_i \quad (12)$$

$$= g(\tau) - (\mathbf{d}_i \circ \phi_i)^T (w_1'^2 - w_1^2) \mathbf{u}_1 \mathbf{u}_1^T \phi_i,$$

where $g(\tau)$ is the gradient in the case of w_1 . Now notice that $g(\tau) = 0$, $\mathbf{u}_1 \mathbf{u}_1^T = \frac{1}{N} \mathbf{1}_{N \times N}$ and both $\mathbf{d}_i \circ \phi_i$ and ϕ_i are nonnegative vectors. This implies $g'(\tau) < 0$ and completes the proof. ■

The above proposition shows the tradeoff between the smoothness and locality, and one can tune the value of w_1 to achieve the desired resolution. The proposed method can be generalized to all differentiable decay functions, but to avoid hindering the clarity of presentation, we focus on the exponential windows.

4. NUMERICAL RESULTS

In this section we evaluate the performance of our proposed framework in revealing vertex-frequency information, through synthetic and real-world graphs.

Undirected graph. Inspired by [18], we consider a random graph composed of three highly connected components (clusters). The graph in Fig. 2 has $N = 60$ nodes, where the first 20 nodes are within the first cluster, the next 20 vertices form the second cluster, and the third cluster comprises the last 20 nodes. We draw an undirected edge (u, v) with probability p_1 if u and v are in the same cluster, and otherwise with probability $p_2 \ll p_1$. In this example, $p_1 = 0.5$ and $p_2 = 0.05$.

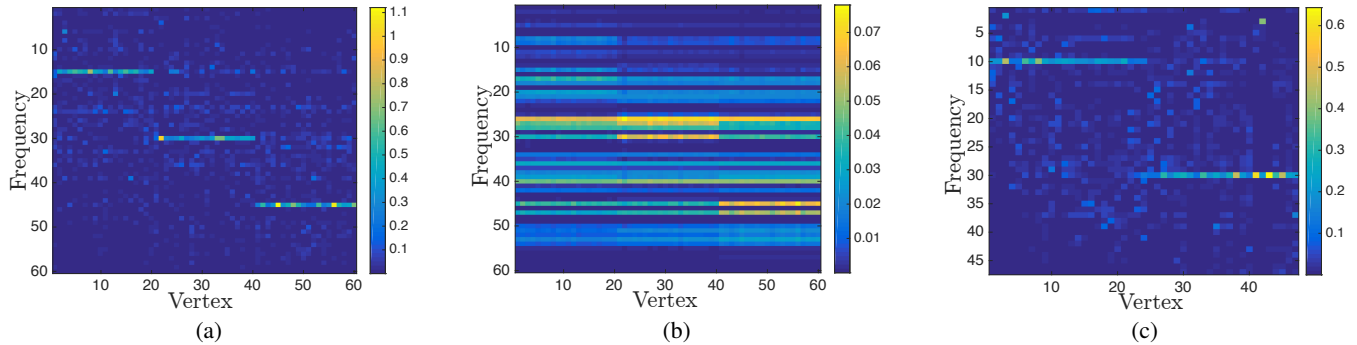


Fig. 1: Spectrograms for both undirected and directed examples: (a) our proposed windowed graph Fourier transform for the graph in Fig. 2 and a signal constructed by three different basis vectors using DGFT in Section 2.2. (b) method in [18] for the same graph and a signal constructed by three different eigenvectors of the Laplacian matrix. (c) our proposed method for the (directed) brain graph.

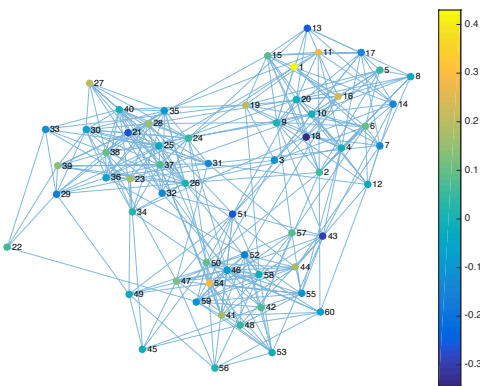


Fig. 2: Synthetic random graph with $N = 60$ nodes containing 3 clusters of size 20 along with a signal constructed by three different basis signals restricted to these clusters.

We obtain a spread Fourier basis $\mathbf{U} = [\mathbf{u}_1, \dots, \mathbf{u}_{60}]$ as described in Section 2.2; see (5). An off-the-shelf algorithm like Dijkstra can be used to find the lengths of all pairs shortest paths and form the proximity matrix \mathbf{D} . Then we solve the optimization problem (8) to learn window parameters $\boldsymbol{\tau}$ via the gradient descent method described in Section 3; see update rule (11). As stated before, we can do so by solving $N = 60$ independent subproblems. Fig. 3 shows the objective functions $f_i(\tau_i)$ in (9) for a subset of $\{1, 2, \dots, N\}$. The positive local minimas in Fig. 3 further corroborate the implications of Proposition 2.

Regarding the signal, we construct the vector \mathbf{x} by adding the following signals: \mathbf{u}_{15} restricted to the first 20 nodes, \mathbf{u}_{30} restricted to the middle 20 nodes, and \mathbf{u}_{45} restricted to the last 20 nodes.

Upon learning decay rates $\boldsymbol{\tau}$ and thus windows, we calculate WGFT of \mathbf{x} , $\tilde{\mathbf{X}}$, in (7). Fig. 1-(a) shows the spectrogram of the signal \mathbf{x} , i.e., the squared magnitude of the elements in $\tilde{\mathbf{X}}$. Not only do the three bold lines in this figure show the transition points where the signal changes, but also they determine the dominant frequency components in each cluster of the graph, namely 15th, 30th, and 45th basis vectors. We compare our result with the method proposed in [18] shown in Fig. 1-(b), where we again construct the signal by concatenating three basis vectors, but this time from $\mathbf{V} = [\mathbf{v}_1, \dots, \mathbf{v}_N]$, eigenvectors of the Laplacian matrix. Although our method significantly outperforms in this case, it is worth mentioning that the performance of [18] improves as we decrease p_2 , i.e., for graphs with more isolated clusters.

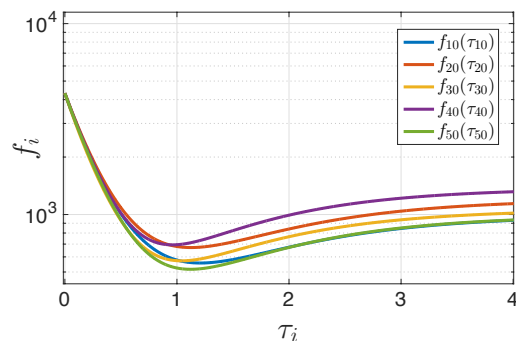


Fig. 3: The objective functions $f_i(\tau_i)$ in (9) for different vertices versus the exponent of the decay function τ_i . The windows corresponding to 5 nodes are illustrated as examples.

Directed graph. We now consider a real brain graph representing the anatomical connections of the macaque cortex, which was studied e.g. in [1, 22]. The network consists of $N = 47$ nodes and 505 edges (among which 121 links are directed). The vertices represent different hubs in the brain, and the edges capture directed information flow among them. We partition the nodes into two highly connected components and similar to the previous experiment, we set the signal in each component to be a different basis vector restricted to that component. In particular, we use the 5th and 35th basis vectors obtained from (5). We also use the lengths the (directed) shortest paths to form matrix \mathbf{D} . Fig. 1-(c) shows the resulting spectrogram using our proposed approach which effectively uncovers the frequency content of each partition, and demonstrates the effectiveness of the put forth windowed digraph Fourier transform.

5. CONCLUSION

In this paper, we introduced the notion of localized graph signal in the vertex domain. Inspired by the traditional short-time Fourier transform, we aimed at finding smooth windows to perform vertex-frequency analyses and infer spectral content of the signal around prescribed vertices in the graph. We tested the effectiveness of the proposed approach through numerical experiments on synthetic and real-world graphs.

With regards to future directions, analyzing the spectral content of the windowed signal is an interesting open question. This is not as easy as in the classical short-time Fourier transform due to the lack of shift-based convolution. Additionally, generalizing the proposed framework to a wider class of windows is a valuable extension.

6. REFERENCES

- [1] Christopher J. Honey, Rolf Kötter, Michael Breakspear, and Olaf Sporns, "Network structure of cerebral cortex shapes functional connectivity on multiple time scales," *Proceedings of the National Academy of Sciences*, vol. 104, no. 24, pp. 10240–10245, 2007.
- [2] Weiyu Huang, Leah Goldsberry, Nicholas F. Wymbs, Scott T. Grafton, Danielle S. Bassett, and Alejandro Ribeiro, "Graph frequency analysis of brain signals," *IEEE Journal of Selected Topics in Signal Processing*, vol. 10, no. 7, pp. 1189–1203, 2016.
- [3] Antonio G. Marques, Santiago Segarra, Geert Leus, and Alejandro Ribeiro, "Sampling of graph signals with successive local aggregations," *IEEE Transactions on Signal Processing*, vol. 64, no. 7, pp. 1832–1843, 2016.
- [4] David I. Shuman, Sunil K. Narang, Pascal Frossard, Antonio Ortega, and Pierre Vandergheynst, "The emerging field of signal processing on graphs: Extending high-dimensional data analysis to networks and other irregular domains," *IEEE Signal Processing Magazine*, vol. 30, no. 3, pp. 83–98, 2013.
- [5] Aliaksei Sandryhaila and José M. F. Moura, "Discrete signal processing on graphs," *IEEE Transactions on Signal Processing*, vol. 61, no. 7, pp. 1644–1656, 2013.
- [6] Oguzhan Teke and Palghat P. Vaidyanathan, "Extending classical multirate signal processing theory to graphs-Part I: Fundamentals," *IEEE Transactions on Signal Processing*, vol. 65, no. 2, pp. 409–422, 2017.
- [7] Oguzhan Teke and Palghat P. Vaidyanathan, "Extending classical multirate signal processing theory to graphs-Part II: M-channel filter banks," *IEEE Transactions on Signal Processing*, vol. 65, no. 2, pp. 423–437, 2017.
- [8] Nicolas Tremblay, Paulo Gonçalves, and Pierre Borgnat, "Design of graph filters and filterbanks," 2017.
- [9] Siheng Chen, Rohan Varma, Aliaksei Sandryhaila, and Jelena Kovačević, "Discrete signal processing on graphs: Sampling theory," *IEEE Transactions on Signal Processing*, vol. 63, no. 24, pp. 6510–6523, 2015.
- [10] Nathanaël Perraudin and Pierre Vandergheynst, "Stationary signal processing on graphs," *IEEE Transactions on Signal Processing*, vol. 65, no. 13, pp. 3462–3477, July 2017.
- [11] Abolfazl Hashemi, Rasoul Shafipour, Haris Vikalo, and Gonzalo Mateos, "Accelerated greedy sampling of graph signals: A weak submodular optimization framework," *IEEE Transactions on Signal Processing*, 2018, (revised; see also arXiv:1807.07222 [eess.SP]).
- [12] Antonio G. Marques, Santiago Segarra, Geert Leus, and Alejandro Ribeiro, "Stationary graph processes and spectral estimation," *IEEE Transactions on Signal Processing*, vol. 65, no. 22, pp. 5911–5926, Nov. 2017.
- [13] Rasoul Shafipour, Santiago Segarra, Antonio G. Marques, and Gonzalo Mateos, "Identifying the topology of undirected networks from diffused non-stationary graph signals," *IEEE Transactions on Signal Processing*, 2018, (revised; see also arXiv:1801.03862 [eess.SP]).
- [14] Santiago Segarra, Gonzalo Mateos, Antonio G. Marques, and Alejandro Ribeiro, "Blind identification of graph filters," *IEEE Transactions on Signal Processing*, vol. 65, no. 5, pp. 1146–1159, 2017.
- [15] Dorina Thanou, David I. Shuman, and Pascal Frossard, "Learning parametric dictionaries for signals on graphs," *IEEE Transactions on Signal Processing*, vol. 62, no. 15, pp. 3849–3862, 2014.
- [16] Xiaofan Zhu and Michael Rabbat, "Approximating signals supported on graphs," in *IEEE International Conference on Acoustics, Speech and Signal Processing (ICASSP)*, 2012, pp. 3921–3924.
- [17] Rasoul Shafipour, Ali Khodabakhsh, Gonzalo Mateos, and Evdokia Nikolova, "A directed graph Fourier transform with spread frequency components," *IEEE Transactions on Signal Processing*, vol. 67, no. 4, pp. 940–960, 2019.
- [18] David I Shuman, Benjamin Ricaud, and Pierre Vandergheynst, "Vertex-frequency analysis on graphs," *Applied and Computational Harmonic Analysis*, vol. 40, no. 2, pp. 260–291, 2016.
- [19] Ljubisa Stankovic, Milos Dakovic, and Ervin Sejdic, "Vertex-frequency analysis: A way to localize graph spectral components," *IEEE Signal Processing Magazine*, vol. 34, no. 4, pp. 176–182, 2017.
- [20] Benjamin Girault, Paulo Gonçalves, and Éric Fleury, "Translation on graphs: An isometric shift operator," *IEEE Signal Processing Letters*, vol. 22, no. 12, pp. 2416–2420, 2015.
- [21] Rasoul Shafipour, Ali Khodabakhsh, Gonzalo Mateos, and Evdokia Nikolova, "Digraph Fourier transform via spectral dispersion minimization," in *Proc. Int. Conf. Acoustics, Speech, Signal Process.*, Calgary, Alberta, Canada, Apr. 15–20, 2018, pp. 6284–6288.
- [22] Mikail Rubinov and Olaf Sporns, "Complex network measures of brain connectivity: Uses and interpretations," *Neuroimage*, vol. 52, no. 3, pp. 1059–1069, 2010.